P1.9

APPLICATIONS OF SYNTHETIC GOES-R OBSERVATIONS FOR MESOSCALE WEATHER ANALYSIS AND FORECASTING

Jack Dostalek*, Lewis Grasso, Manajit Sengupta
Cooperative Institute for Research in the Atmosphere, Colorado State University, Fort Collins, Colorado

Mark DeMaria
NOAA/NESDIS, Fort Collins, Colorado

1. INTRODUCTION

One of the most important advantages of Geostationary Operational Environmental Satellite-R (GOES-R) will be the high time resolution of the observations. It is unlikely that any satellite will be able to provide this type of data on a regular basis prior to the launch of GOES-R. For this reason, synthetic observations are being generated from a numerical cloud model (Colorado State University/Regional Atmospheric Modeling System: CSU/RAMS) in combination with an observational operator that contains radiative transfer algorithms. The emphasis of this work is on product development for mesoscale weather forecasting. Some of the cases that are being simulated by RAMS:

•Oklahoma severe weather outbreak of 8-9 May 2003
•Lake effect snow event of 12-13 February 2003
•Hurricane Lili from 30 September-3 October 2002
•Hurricane Isabel of 11-13 September 2003
•Western fog event of 12 January 2004

2. RAMS OVERVIEW

The numerical cloud model used for this study was RAMS version 4.3 (Pielke et al. 1992). The following features of RAMS were used to simulate the mesoscale weather events:

•The model was run non-hydrostatic and compressible (Tripoli and Cotton 1982).
•Momentum was advanced using a leapfrog scheme while scalars were advanced using a forward scheme. Both methods used second order advection.
•Vertical and horizontal turbulence coefficients were parameterized using the Smagorinsky (1963) deformation based eddy viscosity with stability modifications (Lilly 1962).
• The following hydrometeor species were included in the simulation: Cloud droplets, rain droplets, aggregates, graupel, hail, snow, and pristine ice. Both graupel and hail are mixed phased; that is, liquid water may exist on the surface of each particle. Snow and pristine ice are each divided into five habit categories: columns, hexagonal, dendrites, needles, and rosetta. The mass mixing ratio and number concentration were prognosed using a two-moment bulk microphysical scheme (Meyers et al. 1997) for all hydrometeor types except cloud droplets. The cloud droplet mass mixing ratio was predicted using a one-moment scheme. (Work is ongoing to include cloud droplets into the two-moment scheme.) For all species, the mean diameter was diagnosed.
•Other prognostic variables were the three components of velocity, perturbation Exner function, total water, and ice-liquid potential temperature, (Tripoli and Cotton 1981).
•RAMS uses the Arakawa fully staggered C grid (Arakawa and Lamb 1981).
•Perturbation Exner function tendencies, used to update the momentum variables, were computed using a time split scheme similar to Klemp and Wilhelmson (1978).
•Lateral boundaries used the Klemp-Wilhelmson condition; that is, the normal velocity component specified at the lateral boundary is effectively advected from the interior.
•A wall with friction layers was specified at the top boundary.
•The Land Ecosystem Atmospheric Feedback model, version 2 (Walko et al. 2000) was employed.

3. OBSERVATIONAL OPERATOR OVERVIEW

The observational operator used for computing brightness temperatures was developed at the Cooperative Institute for Research in the Atmosphere (Greenwald et al. 2002). It consists of three main components: radiative transfer models, hydrometeor optical (or single-scatter) property models, and a gas extinction model. The specific components are:

•The radiative transfer model at infrared wavelengths uses the Delta-Eddington 2-stream method (Deeter and Evans 1998).
•The radiative transfer model at solar wavelengths uses the spherical harmonic discrete ordinate method (Evans 1998).
•Cloud optical properties at all wavelengths are based on anomalous diffraction theory (Mitchell 2000; Mitchell 2002; Greenwald et al. 2002) applied to both liquid and ice particles.
•The gas extinction at all wavelengths is based on the OPTRAN radiative transfer model (McMillin et al. 1995).

4. SYNTHETIC/REAL GOES COMPARISONS

As a first test of the RAMS/observational operator modeling approach, the severe weather and lake effect snow cases were simulated. Synthetic GOES 10.7 μm imagery was created and compared with real GOES

* Corresponding author address: Jack Dostalek, 1375 Campus Delivery; Fort Collins, CO 80523-1375.
email: dostalek@cira.colostate.edu.

imager data. Figs. 1 and 2 show examples of the comparison for each case. Although the model forecasts are not perfect, the real and synthetic imagery are qualitatively similar. Further, the imagery shows similar ranges of spatial variability of the brightness temperatures. This comparison provides some confidence that inferences made from the synthetic data will be applicable to real GOES-R observations when they become available.

5. HES RESOLUTION IMPACT STUDY

The GOES-R Hyperspectral Environmental Suite (HES) sounder will have much improved spatial and vertical resolution relative to the current GOES sounder. For severe weather applications, the improved spatial resolution (4 km versus 10 km) will provide more views of cloud-free areas. As a first test of the utility of the HES, synthetic Derived Product Imagery (DPI) of Convective Available Potential Energy (CAPE) was created for two hours of the severe weather simulation from the inner-most grid that had 1 km horizontal grid spacings. Shown in Fig. 3 is a comparison of the synthetic DPI for spatial footprints of 50, 30, 10, and 4 km. The 50, 30 and 10 km plots are similar to what is available from the current GOES, which uses 5x5, 3x3, or 1x1 10 km fields of view. The 4 km DPI reveals considerably more structure compared to the larger footprint images. Fig. 4 shows the percentage of cloud-free areas for a two hour simulation of the entire domain of the inner-most grid, including 1 km footprint DPI CAPE imagery. With smaller footprints, a larger fraction of the cloud-free area can be viewed.

6. FUTURE PLANS

The numerical model/radiative transfer simulations will be performed for the other case studies. Synthetic GOES-R imager data will be generated for mesoscale product development. Data assimilation studies will first be performed using an identical twin approach, followed by real-data tests with AIRS and other hyperspectral IR data sets. In the longer term, RAMS will be replaced by the Weather Research and Forecasting (WRF) model to increase collaboration with operational forecasting centers.

Acknowledgments. This material is based on work supported by the National Oceanic and Atmospheric Administration under Grant NA67RJ0152. The views, opinions, and findings in this report are those of the authors, and should not be construed as an official NOAA and or U.S. Government position, policy, or decision.

7. REFERENCES

Arakawa, A., and V. Lamb, 1981: A potential enstrophy and energy conserving scheme for the shallow water equations. *Mon. Wea. Rev.,* **109**, 18-36.

Evans, K. F., 1998: The spherical harmonics discrete ordinate method for three-dimensional atmospheric radiation transfer. *J. Atmos. Sci.,* **55**, 429-446.

Deeter, M., and K. F. Evans, 1998: A hybrid Eddington-single scatter radiative transfer model for computing radiances from thermally emitting atmospheres. *J. Quant. Spect. Rad. Transfer,* **60**, 635-648.

Greenwald, T. J., R. Hertenstein, and T. Vukicevic, 2002: An all-weather observational operator for radiance data assimilation with mesoscale forecast models. *Mon. Wea. Rev.,* **130**, 1882-1897.

Klemp, J. B. and R. B. Wilhelmson, 1978: The simulation of three-dimensional convective storm dynamics. *J. Atmos. Sci.,* **35**, 1070-1096.

Lilly, D. K., 1962: On the numerical simulation of buoyant convection. *Tellus,* **14,** 148-172.

McMillin, L. M., L. J. Crone, M. D. Goldberg, and T. J. Kleespies, 1995: Atmospheric transmittance of an absorbing gas, 4. OPTRAN: A computationally fast and accurate transmittance model for absorbing gases with fixed and variable mixing ratios at variable viewing angles. *Appl. Opt.,* **34**, 6269-6274.

Meyers, M. P., R. L. Walko, J. Y. Harrington, and W. R. Cotton, 1997: New RAMS cloud microphysics parameterization. Part II: The two-moment scheme. *Atmos. Res,* **45**, 3-39.

Mitchell, D. L., 2000: Parameterization of the Mie extinction and absorption coefficients for water clouds. *J. Atmos. Sci.,* **57**, 1311-1326

Mitchell, D. L., 2002: Effective diameter in radiation transfer: General definitions, applications, and limitations. *J. Atmos. Sci.,* **59**, 2330-2346.

Pielke, R. A., W. R. Cotton, R. L. Walko, C. J. Tremback, W. A. Lyons, L. D. Grasso, M. E. Nicholls, M. D. Moran, D. A. Wesley, T. J. Lee, J. H. Copeland, 1992: A comprehensive meteorological modeling system-RAMS. *Meteor. and Atmos. Phys.,* **49**, 69-91.

Smagorinsky, J., 1963: General circulation experiments with the primitive equations. Part 1: The basic experiment. *Mon. Wea. Rev.,* **91**, 99-164

Tripoli, G. J., and W. R. Cotton, 1981: The use of ice-liquid water potential temperature as a thermodynamic variable in deep atmospheric models. *Mon. Wea. Rev.,* **109**, 1094-1102.

Tripoli, G. J., and W. R. Cotton, 1982: The Colorado State University three dimensional cloud mesoscale model,1982. Part I: General theoretical framework and sensitivity experiments. *J. Rech. Atmos.,* **16**, 185-220.

Walko, Robert L., L. E. Band, J. Baron, T. Kittel, G. F., R. Lammers, T. J. Lee, D. Ojima, R. A. Pielke, C. Taylor, C. Tague, C. J. Tremback, and P. L. Vidale, 2000: Coupled Atmosphere-Biophysics-Hydrology Models for Environmental Modeling. *J. Appl. Meteor.,* **39**, 931-944.

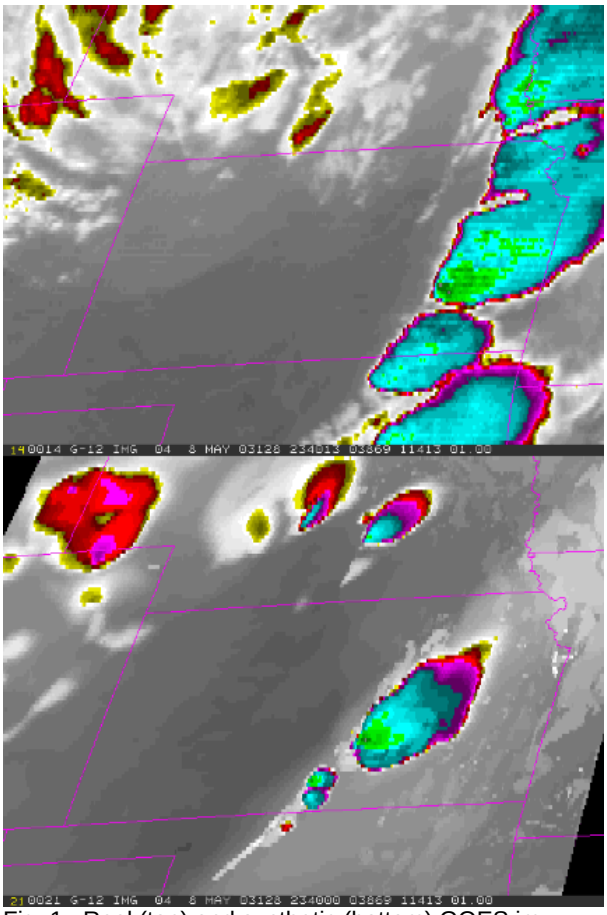

Fig. 1. Real (top) and synthetic (bottom) GOES imagery for the 8 May 2003 severe weather event.

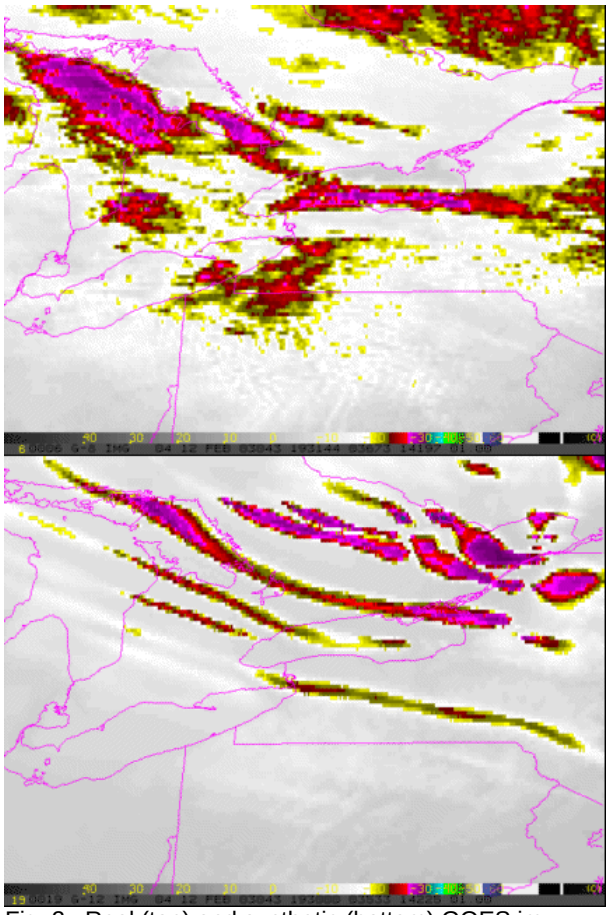

Fig. 2. Real (top) and synthetic (bottom) GOES imagery for the 12 February 2003 lake effect snow event.

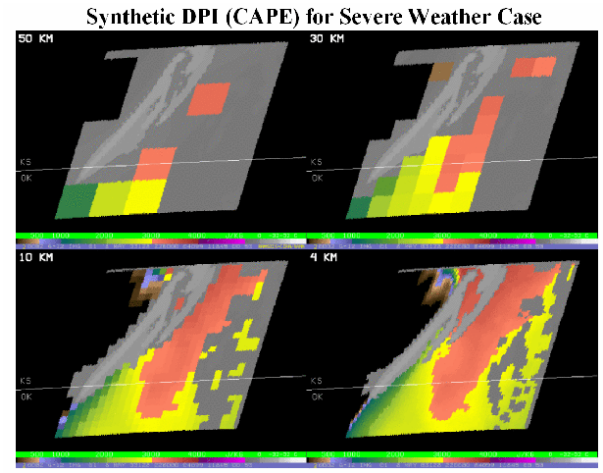

Fig. 3. Example of a DPI CAPE product with 50, 30, 10, and 4 km footprints. The DPI is calculated in regions of cloud free footprints in the simulated domain

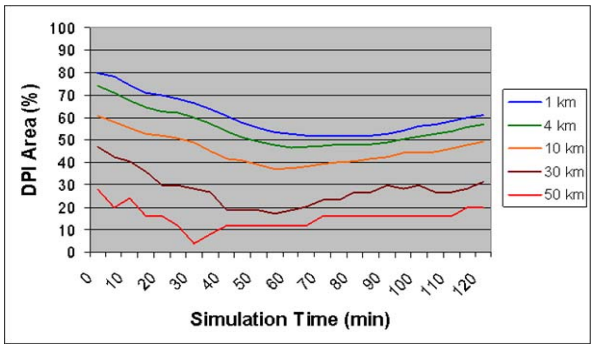

Fig. 4. The percent of the innermost simulated domain that is cloud free when divided into footprints of 50, 30, 10, 4, and 1 km. Each area must be completely cloud free to be in the cloud-free percentage.